Magnetic Structure of Mn-Deficient $LaMn_{1-x}Sb_2$

The magnetic structure of $RMPn_2$ compounds could be the critical factor for the electronic band structure and topologic properties.

The magnetic order and nontrivial electronic structures coexist in the layered $RMPn_2$ (R = rare earth, M = transition metal, Pn = Sb or Bi) magnetic topological semimetals. Most of the $RMPn_2$ compounds exhibit metallic conduction behaviors, and both antiferromagnetic (AFM) and ferromagnetic ground states can be realized in different systems with various R and Pn ions or ion vacancies. The Ruderman–Kittel–Kasuya–Yosida (RKKY) interactions are crucial in the compounds and account for the correlation between the magnetic order and electronic states. It has been suggested that the topologically nontrivial electronic band structure could be related to the magnetic order. The G-type AFM could stabilize a line node in the electronic band,[1] whereas the C-type structure stabilizes a gapped Dirac state.[2] Furthermore, a canted C-type structure is found to possess topologically protected Weyl nodes.[3] In the magnetic topological semimetals research, the neutron diffraction technique could provide valuable information.

Aifeng Wang (Chongqing University, China) and collaborators study the layered $RMSb_2$ with different rare earth ions and Mn occupancies. Recently, Wang and his collaborators published the crystal growth, resistivity, bulk magnetometry, specific heat, and magnetic structure of $LaMn_{1-x}Sb_2$ single crystals. Single-crystal samples were successfully grown using the Sn flux method (inset to **Fig. 1(c)**), and the crystal of the sample was confirmed as a tetragonal $P4/nmm$ structure by X-ray diffraction.

The resistivity, specific heat, magnetization, and the Seebeck coefficient provide evidence of the Néel temperature occurring at T_N~ 172 K, as shown in **Fig. 2**. The $M(T)$ data display magnetic anisotropy and indicate that the easy-axis aligns with the c-axis. The $M(B)$ curves show a spin flop transition with $B//c$, supporting the idea that the easy axis should be along the c axis. Negative magnetoresistance reaches ~10% at a magnetic field of 9 T, whereas an abrupt increase of MR at ~2 T for $B//c$ is observed, as shown in **Fig. 2(f)**. The abrupt change coincides with the spin-flop transition observed in $M(B)$ curves, indicating its magnetic origin.

The high-resolution neutron powder diffractometer **ECHIDNA** at ANSTO was used to collect neutron powder diffraction patterns of the pulverized Sb-flux-grown $LaMn_{0.78}Sb_2$ single crystals. The neutron data revealed the magnetic order, whose observed magnetic peaks can be indexed with a commensurate wave vector k = (0, 0, 1/2), *i.e.*, the magnetic unit cell is twice the size along the c-axis of the structural unit cell. $LaMn_{0.78}Sb_2$ magnetically orders to the G-type magnetic structure with moments aligned along the c-axis, as illustrated in **Fig. 3(b)**. Based on the magnetization and neutron diffraction measurements of $LaMn_{0.78}Sb_2$, the magnetic structure of $LaMn_{0.86}Sb_2$ is likely a canted G-type AFM. First principle calculations, which incorporate the spin-orbital coupling (SOC) for a G-type AFM structure, indicate the presence of Dirac dispersion below the Fermi level. However, the relevant quantum transport properties have not been observed owing to high Fermi energy and the existence of a Mn vacancy. These results[4] indicate that $LaMn_{1-x}Sb_2$ displays vacancy tunable magnetism and Dirac dispersion and could be an attractive topological semimetal candidate via proper adjusting of the Fermi energy and Mn vacancies. Further studies of putative Dirac states and their interaction with magnetism could be intriguing for future studies.[5] (Reported by Chin-Wei Wang)

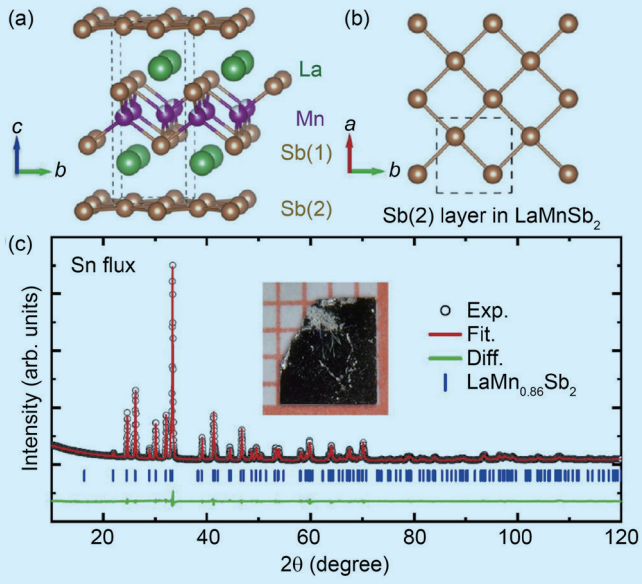

Fig. 1: (a) The crystal structure of $LaMn_{1-x}Sb_2$ of the tetragonal $P4/nmm$ structure, in which Sb(1) and Sb(2) denote the Sb bonded with Mn and Sb, respectively. (b) Top view of the Sb(2) square net. (c) Refined X-ray powder diffraction (XRPD) pattern for $LaMn_{0.86}Sb_2$. The inset shows a photograph of a $LaMn_{0.86}Sb_2$ single crystal. [Reproduced from Ref. 4]

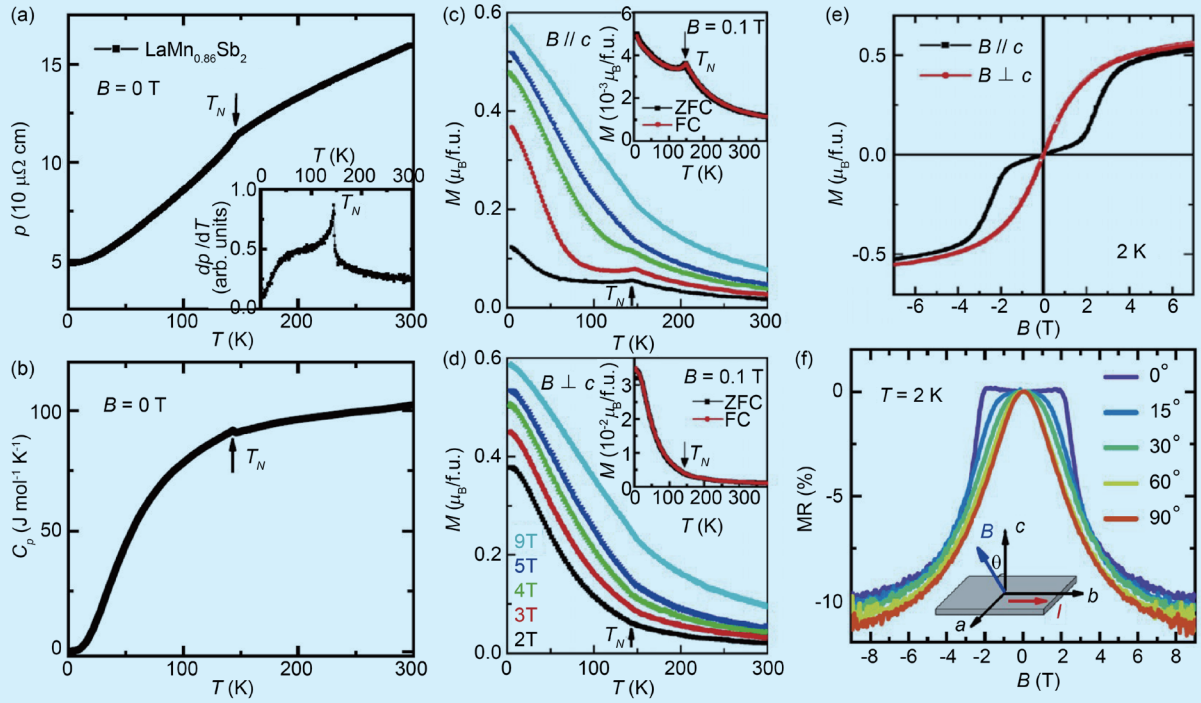

Fig. 2: (a) Temperature dependence of in-plane resistivity for a $LaMn_{0.86}Sb_2$ single crystal; the inset shows the first derivative of resistivity with respect to temperature d$\rho(T)$/dT. (b) Temperature dependence of specific heat $C_p(T)$. Temperature-dependent magnetization $M(T)$ at various magnetic fields up to 9 T for both B//c (c) and $B\perp c$ (d). The insets show the data of B = 0.1 T. (e) $M(B)$ curve collected at 2 K with B//c and $B\perp c$. (f) Magnetic field dependence of MR with field gradually tilted away from c-axis. [Reproduced from Ref. 4]

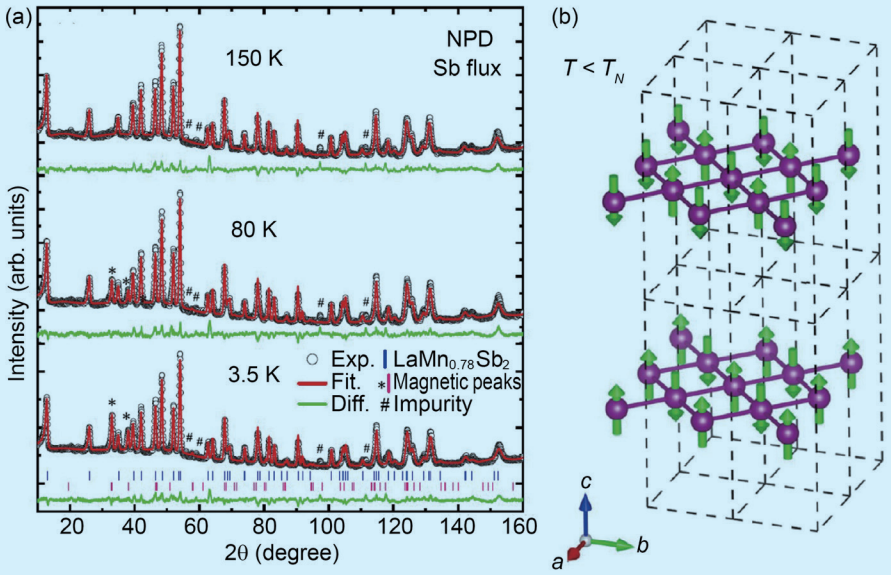

Fig. 3: (a) Refined neutron powder diffraction (NPD) patterns at various temperatures. (b) The magnetic structure deduced from the NPD result, where the dashed line represents the crystallographic unit cells. The magnetic unit cell is doubled along the c-axis of the crystallographic unit cell. [Reproduced from Ref. 4]

This report features the work of Aifeng Wang and his collaborators published in Phys. Rev. B ***107****, 115150 (2023).*

ANSTO ECHIDNA – High-resolution Powder Diffractometer

- NPD
- Materials Science, Chemistry, Condensed-matter Physics

References

1. Z. Qiu, C. Le, Z. Liao, B. Xu, R. Yang, J. Hu, Y. Dai, X. Qiu, Phys. Rev. B **100**, 125136 (2019).
2. R. Kealhofer, S. Jang, S. M. Griffin, C. John, K. A. Benavides, S. Doyle, T. Helm, P. J. W. Moll, J. B. Neaton, J. Y. Chan, J. D. Denlinger, J. G. Analytis, Phys. Rev. B **97**, 045109 (2018).
3. Y.-Y. Wang, S. Xu, L.-L. Sun, T.-L. Xia, Phys. Rev. Mater. **2**, 021201(R) (2018).
4. T. Yang, L. Zhang, C.-W. Wang, F. Gao, Y. Xia, P. Jiang, L. Zhang, X. Mi, M. He, Y. Chai, X. Zhou, H. Fu, W. Ren, A. Wang, Phys. Rev. B **107**, 115150 (2023).
5. T. J. Slade, A. Sapkota, J. M. Wilde, Q. Zhang, L.-L. Wang , S. H. Lapidus, J. Schmidt, T. Heitmann, S. L. Bud'ko, P. C. Canfield, Phys. Rev. Mater. **7**, 114203 (2023).